



A Comprehensive Investigation of Solvatochromism and Solvation in Medicinally Significant Sulfa Drugs: Estimation of Excited State Dipole Moments

Vibha K*, Prachalith N C*, Suresh Kumar H. M.†, Ravikantha M. N‡, Annoji Reddy R• and Thipperudrappa J*

Abstract

The solvatochromic properties of important sulfa drug molecules sulfadiazine (SDZ), sulfamerazine (SMZ) and sulfamethazine (STZ) were investigated in solvents of different polarities, including their solvation in a binary THF-Water solvent mixture. Steady-state absorption and fluorescence methods were utilized to analyse the absorption and fluorescence spectra of these compounds which reveals the significant spectral shifts corresponding to changes in solvent polarity. Further insights on the solvatochromic characteristics of the examined drug molecules were obtained using Lippert-Mataga, Reichardt's, Kamlet-Taft, and Catalan's solvent polarity approaches. The study also identified synergistic effects in the THF-Water solvent mixture. Different solvatochromic techniques were employed to calculate the excited-state dipole moment of the studied molecules. The Bilot-Kawaski approach was utilized to investigate

* Department of Physics, Vijayanagara Sri Krishnadevaraya University, Ballari - 583 105, India; vibhakarkihalli@gmail.com, prachalithn@gmail.com, jtrphy2007@gmail.com

† Department of Physics, Siddaganga Institute of Technology, Tumakuru, Karnataka- 572103. India; sureshkumarhm@gmail.com

‡ Department of Physics, Government Science College, Chitradurga-577 501, India; ravikanthmn@gmail.com

• Department of Physics, GVVP GFGC, Hagari Bommanahalli-583 212, India; anojphy123@gmail.com

the influence of solute polarizability on the excited state dipole moment and the change in dipole moment.

Keywords: Dipole moment, Polarizability, Preferential solvation, Solvatochromic, Sulfa drugs.

1. Introduction

Sulfadiazine (SDZ), Sulfamerazine (SMZ) and sulfamethazine (STZ) belong to the group of sulfonamides and are also called sulfa drugs. Sulfa drugs contain a sulfur atom connected with two sets of double-bonded oxygen atoms, a side chain of carbon and nitrogen atom bonded to the sulfur atom itself. To the sulfonamide group, pyrimidine, methyl-pyrimidine and dimethyl-pyrimidine groups are attached in SDZ, SMZ, and STZ molecules respectively. Sulfonamide derivatives have expanded their applications in analytical chemistry due to their promising sensing properties used in environmental, forensic, and biochemistry laboratories [1,2] and are used in various medical fields. Mainly they are used to cure numerous infections caused by gram-negative/positive microorganisms [3], urinary tract infections [4], treat different forms of pneumonia and malaria in AIDS/HIV patients [5] and, in animal/human therapy [6]. In the resources of veterinarians and physicians [7], sulfa drugs also occupy a vital place.

The fluorescence features of different sulfa drugs have been reported [8,9]. Using the fluorescamine reaction, the analysis of sulfa drugs has been achieved in pharmaceuticals and foods [10]. The sulfa-drugs were estimated in the preparation of milk and pharmaceuticals by using photochemically-induced fluorometry [11]. These applications and studies on sulfa drug molecules have indicated the importance of the fluorescence features of these molecules. The utilization of sulfa drugs in various applications, specifically in fluorescence-based applications, necessitates an exploration of their photophysical characteristics including absorption and fluorescence in different environments. The present investigation is focussed mainly on these aspects of sulfa drug molecules. Fluorescence spectroscopy is an excellent research tool to investigate photophysical characteristics of a fluorophore [12-15]. In the recent past, the investigation of

photophysical characteristics of various fluorophores has been a topic of numerous investigations [16-28].

Further, solvatochromism which is based on absorption and fluorescence shifts plays a dynamic role in research and is considered as an important proof for the intramolecular charge transfer (ICT) occurring in the molecules. Also, the solvatochromic shift method is used to find the type of electronic transition taking place in the fluorophore. The dipole moment of a fluorophore gives prodigious insight into the fluorophore's molecular structure and relocation of electronic charge. The difference in the ground and excited state dipole moment gives information about the interactions that occur between fluorophore and solvent. The dipole moment in the excited state gives evidence of various relaxation mechanisms occurring in the excited state. The correlation (linear) between solvatochromic shift and polarity of solvent is used to calculate the excited state dipole moment. Several methods were used to estimate the ground/excited state dipole moment namely Lippert-Mataga [29,30], Bilot-Kawski [31], Bakhshiev's [32], Kawski-Chamma-Viallet [33,34] and Reichardt's solvent polarity parameter at microscopic level [35]. Kamlet and Catalan methods were used to explain the impact of specific solvent parameters on absorption and fluorescence characteristics of fluorescent molecules [36-38].

The preferential solvation (PS) is a subject of current interest, which involves the dissolution of a solute molecule in binary solvents [39-41]. The behaviour of sulfa drugs in the co-solvent mixture has been frequently estimated for the pre-formulation and purification design of liquid medicine. Experimental studies suggest that solute may persuade a change in the composition of solvent in the sphere of solvation than that in the bulk [42,43]. In PS the solute (fluorophore) is preferentially solvated by one of the solvents due to solvent-solvent/solute-solvent interaction. Therefore, due to preferential solvation solute-solvent interaction complexity is higher in binary mixture than that of neat solvent. For instance, in a binary mixture of THF-Water, the interaction between the THF-Water is relatively weaker than the water-water interaction at a low concentration of THF [44]. The literature reports the spectroscopic investigation and preferential solvation study of a few sulfa drugs [45,46].

Recently, we have reported the computational studies on SDZ, SMZ and STZ drug molecules by density functional theory [47]. In continuation of our previous work, in the present investigation solvatochromism, solvation and dipole moment studies have been carried out. To the best of our knowledge, this is the first report on the detailed study on solvatochromism, solvation and estimation of dipole moments using various solvatochromism approaches in neat and mixed solvents. The experimental results are analysed using the Lippert-Mataga (LM) bulk solvent polarity parameter, Reichardt's microscopic solvent polarity parameter (E_N^T) and the solvatochromic parameters proposed by Kamlet and Catalan. Also, the preferential solvation study on these molecules is carried out in the THF-Water binary mixture. The estimation of the dipole moments in the excited state was carried out using Bakhshiev's and Bilot-Kawski's relation and the formula derived from E_N^T in pure solvents. The dipole moments in the ground and excited states also have been computed using DFT and TD-DFT calculations in a vacuum.

2. Materials and Methods

2.1. Materials

SDZ, SMZ and STZ molecules (99% purity) have been purchased from Sigma-Aldrich. They are used further without any purification. The structural arrangement of sulfa drugs is depicted in Fig. 1. The solvents utilized in this study are of spectroscopic-grade quality and were obtained from S.D. Fine Chemical Ltd., India. The doubled distilled water was used for solvation studies. The dielectric constant, refractive index and E_N^T values for various solvents are sourced from existing literature [35].

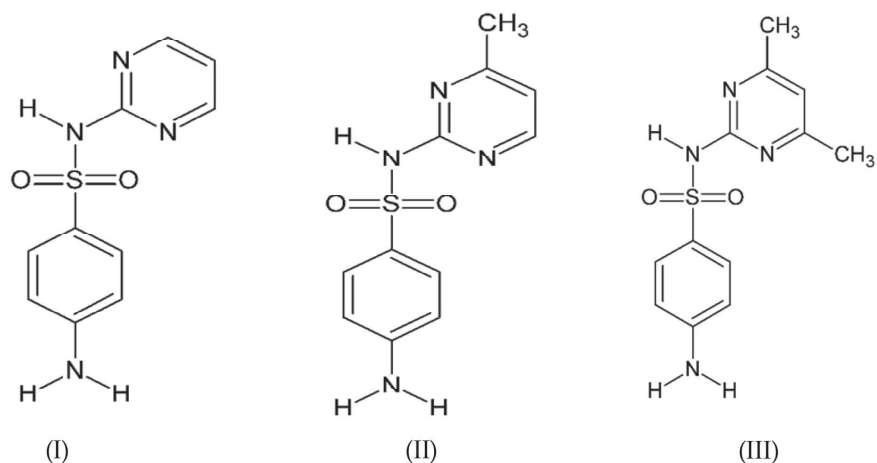


Fig. 1. The molecular structure of (I) SDZ (II) SMZ and (III) STZ molecules.

2.2. Experimental and Computational Methods

The UV-Vis absorption spectra were taken within the range of 200-500 nm using a UV-Vis spectrophotometer (LABINDIA, Model: UV-3092). The fluorescence spectra were recorded using a spectrofluorometer (Agilent, U.S.A, Model: Cary Eclipse-3000) in the range of 250-500nm. The concentration of SDZ, SMZ and STZ in all the solvents / solvent mixture was kept low at 5×10^{-5} M to reduce the formation of aggregation and self-absorption. The freshly prepared solutions were utilized for both absorption and emission measurements, which were conducted at ambient room temperature. All the computational calculations on SDZ, SMZ and STZ have been carried out using the Gaussian09 software [48]. To generate input file for Gaussian software and analyse Gaussian output file, Gauss View 6.0 visualization program has been used [49]. The molecular structures of SDZ, SMZ and STZ were optimized using density functional theory at 6-311+G (d, p) basis set with B3LYP level of theory. The TD-DFT with IEEPCM (Integral equation formalism of the polarizable continuum model) has been used to compute absorption spectra in vacuum. The Onsager cavity radius has been calculated using Suppan's equation [50].

3. Theory

3.1. Solvatochromism in Neat Solvents

To analyse solvatochromism in the investigated molecules spectral parameters are correlated with the Lippert-Mataga bulk solvent polarity parameter $\Delta F_{L-M}(\epsilon, n)$ given by Eqn.1 and E_N^T parameter [35].

$$\Delta F_{L-M}(\epsilon, n) = \frac{(\epsilon-1)}{(2\epsilon+1)} - \frac{n^2-1}{2n^2+1} \quad (1)$$

Where all the terms have their usual meanings.

The spectral properties are also analysed using multiple linear regression methods suggested by Kamlet (Eqn.2) and Catalan (Eqn.3).

$$y = y_0 + a\alpha + b\beta + c\pi^* \quad (2)$$

$$y = y_0 + aSA + bSB + cSP + dSdP \quad (3)$$

In this context, 'y' denotes the spectroscopic property being analysed, y_0 represents the spectroscopic in the gas phase, ' α ' signifies the strength of the hydrogen bond donor (HBD), ' β ' denotes the strength of the hydrogen bond acceptor (HBA) and π^* refers to non-specific dielectric interactions. SdP, SP, SA and SB are the solvent dipolarity, solvent polarity, solvent acidity, and solvent basicity respectively. a, b, c and d represent indicators of the impact of solvents HBD/ acidity, HBA/basicity, non-specific dielectric interaction/polarity and dipolarity respectively.

3.2. Preferential Solvation Study

The maximum wavenumber ($\bar{\nu}_{12}$) in an ideal case of the spectroscopic parameter in a binary mixture is given by Eqn. 4.

$$\bar{\nu}_{12} = \bar{\nu}_1 X_1 + \bar{\nu}_2 X_2 \quad (4)$$

Here, X_2 represents the bulk mole fraction of solvent 2 and X_1 represents the bulk mole fraction of solvent 1. $\bar{\nu}_1$ and $\bar{\nu}_2$ denotes the absorption/fluorescence maximum wavenumber of sulfa drugs in solvent 1 and solvent 2 respectively.

The $\bar{\nu}_{12}$ in non-ideal case can be expressed as in Eqn.5

$$\bar{\nu}_{12} = \bar{\nu}_1 X_1^L + \bar{\nu}_2 X_2^L \quad (5)$$

where X_2^L is the local mole fraction of solvent 2 and X_1^L is the local mole fraction of solvent 1 in the cybotatic area of a molecule. The other terms have their usual meanings.

Various solvation parameters are employed to illustrate the preferential solvation of dissolved substances as outlined in Equations (6), (7) and (8).

$$X_2^L = \frac{\bar{v}_{12} - \bar{v}_2}{\bar{v}_2 - \bar{v}_1} = 1 - X_1^L \quad (6)$$

$$K_{sp} = X_2^L \times X_1 / X_1^L \times X_2 \quad (7)$$

$$\delta_{12} = X_2^L - X_1 \quad (8)$$

Where X_2^L and X_1^L retain their previously defined meanings, K_{sp} represents the preferential solvation constant. A K_{sp} value less than 1 indicates a preference for first solvent over second solvent, whereas a K_{sp} value greater than 1 indicates a preference for second solvent over first solvent. δ_{12} represents the preferential solvation index. A negative δ_{12} value indicates a preference for first solvent over second solvent, while a positive δ_{12} value signifies the opposite.

The molar percentage of the hydroxylic component (ROH) for a 1:1 bulk mole fraction in each mixture is calculated using the following Equation 9.

$$\text{ROH (\%)} = (\lambda_{0.5} - \lambda_{0.0}) / (\lambda_{1.0} - \lambda_{0.0}) \times 100 \quad (9)$$

Whereas ROH (%) is the molar % of the hydroxylic component in the binary mixture, $\lambda_{1.0}$, $\lambda_{0.5}$, $\lambda_{0.0}$, are mole fractions equal to 1.0, 0.5, 0.0 respectively corresponding to the peak absorption wavelength (λ_{max}) for the protic solvent.

3.3. Estimation of Ground State Dipole Moment

The ground state dipole moment is determined through computational quantum chemical calculations. These computations were conducted using the Gaussian09 software, employing the B3LYP level of theory and the 6-311+G(d, p) basis set.

3.4. Estimation of Excited State Dipole Moment

The excited state dipole moment (μ_e) of molecules was estimated using the methods suggested by Lippert- Mataga, Bakshiev and

Kawski-Chamma-Viallet. These methods are depicted in the Eqs. (10), (11) and (12) respectively.

$$(\bar{\nu}_a - \bar{\nu}_f) = m_{L-M} F_{L-M}(\epsilon, n) + \text{Constant} \quad (10)$$

$$(\bar{\nu}_a - \bar{\nu}_f) = m_B F_B(\epsilon, n) + \text{Constant} \quad (11)$$

$$\frac{(\bar{\nu}_a + \bar{\nu}_f)}{2} = -m_{K-C-V} F_{K-C-V}(\epsilon, n) + \text{Constant} \quad (12)$$

Here $\bar{\nu}_a$ and $\bar{\nu}_f$ are absorption and fluorescence wavenumber maxima respectively, $F_{L-M}(\epsilon, n)$ (Lippert-Mataga), $F_B(\epsilon, n)$ (Bakhshiev's) and $F_{K-C-V}(\epsilon, n)$ (Kawski-Chamma-Viallet) are polarity function parameters. m_{L-M} (Lippert-Mataga), m_B (Bakhshiev's) and m_{K-C-V} (Kawski-Chamma-Viallet) are respective slopes and are given by Eqs. (13), (14) and (15)

$$m_{L-M} = \frac{2(\mu_e - \mu_g)^2}{hca^3} \quad (13)$$

$$m_B = \frac{2(\mu_e - \mu_g)^2}{hca^3} \quad (14)$$

$$m_{K-C-V} = \frac{2(\mu_e^2 - \mu_g^2)}{hca^3} \quad (15)$$

Where h is Planck's constant, c is the velocity of light and ' a ' is the Onsager cavity radius of the molecule. μ_g and μ_e are ground and excited dipole moments of the molecule respectively. The μ_e can be calculated using Eqs.13-15 by knowing the slope and other terms.

Here, h represents Planck's constant, c denotes the velocity of light, and ' a ' signifies the Onsager cavity radius of the molecule. μ_g and μ_e stand for the ground and excited dipole moments of the molecule, respectively. The μ_e can be determined by utilizing Equations 13-15, with the slope and other relevant terms known.

The μ_e can also be estimated by the method based on empirical solvent polarity parameter E_N^T using the Eqs. (16) and (17)

$$\bar{\nu}_a - \bar{\nu}_f = m_{E_N^T} E_N^T + \text{Constant} \quad (16)$$

$$\text{Where slope } m_{B-K} = \frac{2(\mu_e - \mu_g)^2}{hca^3} \quad (17)$$

where $\Delta\mu_b = 9 D$ is change in dipole moment and $a_b = 6.2 \text{ \AA}$ is Onsager radius of the Betaine dye, and a and $\Delta\mu$ are the equivalent quantities of the respective molecule.

3.5. Effect of Polarizability on Excited State Dipole Moment and Change in Dipole Moment

The effect of polarizability of solute on the excited state dipole moment and change in dipole moment can be realised using the method suggested by Bilot-Kawski [31]. According to this method the Stokes shift ($\bar{\nu}_a - \bar{\nu}_f$) can be written as

$$(\bar{\nu}_a - \bar{\nu}_f) = m_{B-K} F_{B-K}(\epsilon, n) + \text{Constant} \quad (18)$$

Where, m_{B-K} is the slope of the plot ($\bar{\nu}_a - \bar{\nu}_f$) versus $F_{B-K}(\epsilon, n)$ and is given by

$$m_{B-K} = \frac{2(\mu_e - \mu_g)^2}{hc a^3} \quad (19)$$

$F_{B-K}(\epsilon, n)$ is the Bilot-Kawski polarity function and is $F_{B-K}(\epsilon, n)$ is given by Eqn (20)

$$F_{B-K}(\epsilon, n) = \frac{\frac{\epsilon-1}{2\epsilon+1} \frac{n^2-1}{2n^2+1}}{\left(1 - \frac{2\alpha}{a^3} \frac{\epsilon-1}{2\epsilon+1}\right) \left(1 - \frac{2\alpha}{a^3} \frac{n^2-1}{2n^2+1}\right)^2} \quad (20)$$

Here, $2\alpha/a^3$ is the polarizability factor, α is the polarizability of solute, a is the Onsager cavity radius of the solute molecule and other terms have their usual meaning. The excited state dipole moment can be estimated for different values of $2\alpha/a^3$ by using the values of m_{B-K} obtained by plotting the linear correlation of ($\bar{\nu}_a - \bar{\nu}_f$) versus $F_{B-K}(\epsilon, n)$.

4. Results and Discussion

4.1. Solvatochromism in Neat Solvents

The experimental absorption and fluorescence spectra of SDZ, SMZ and STZ were recorded in different solvents having different polarities and are displayed in Fig.2 (a) and Fig.2 (b) respectively. The spectral parameters absorption maxima (λ_a), emission maxima (λ_f) and Stokes shifts ($\Delta\bar{\nu}$) are listed in Table 1. It is noticed that the absorption spectra

shows the hypsochromic (blue) shift of nearly 15nm (blue-shift) when the solvent is switched from toluene (non-polar) to acetonitrile (polar aprotic) in all the molecules. But, when the solvent is switched from toluene to water, the absorption spectra shows the hypsochromic (blue) shift of nearly 23nm in all the molecules. The hypsochromic shift with an increase in the polarity of solvents indicates the $n \rightarrow \pi^*$ type of transition in all these molecules. The $n \rightarrow \pi^*$ type of transition in all these molecules is attributed to nitrogen present in the sulfonamide group. Normally, the n-state is more stabilized in polar solvents than the π^* state as shown in Fig.3. This leads to an increase in the energy difference between the ground and excited state in polar solvents and hence the blue shift.

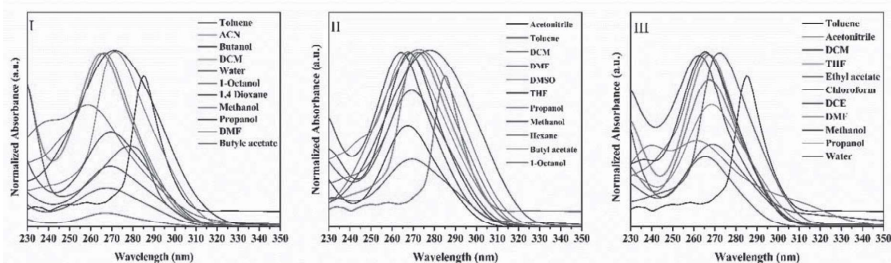


Fig. 2(a). Normalized Absorption spectra of (I) SDZ, (II) SMZ and (III) STZ molecules.

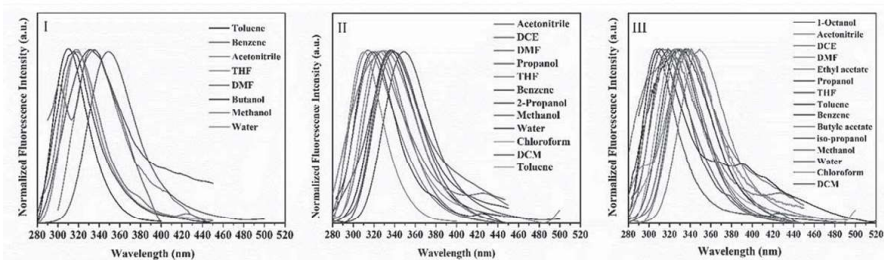


Fig. 2(b). Normalized fluorescence spectra of (I) SDZ, (II) SMZ and (III) STZ molecule

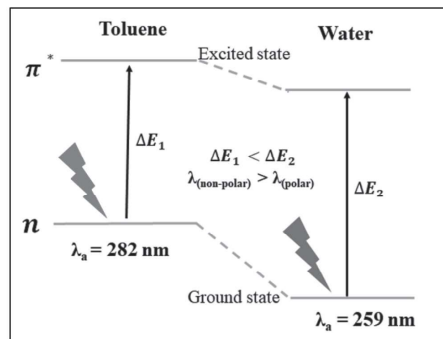


Fig. 3. The $\pi \rightarrow \pi^*$ transition in sulfa drug molecules in Toluene (non-polar) and Water (polar) solvents.

The emission spectra shows the bathochromic (red) shift of nearly 18nm (red-shift) when the solvent is switched from toluene to acetonitrile in all molecules. But, when the solvent is switched from toluene to water, the emission spectra shows a red shift of nearly 30nm in all molecules. This could be due to the formation of hydrogen bond between solute molecules and polar-protic solvents at sulfonyl oxygen [51]. The redshift observed with higher solvent polarity suggests a transition of the $\pi \rightarrow \pi^*$ type in all these molecules. The $\pi \rightarrow \pi^*$ type of transition in all these molecules may attributed due to the presence of conjugated benzene ring and pyrimidine ring in the titled molecules. Normally, π^* - state is more stabilized than π -state in polar solvents as shown in Fig. 4, leading to redshift. Further, the Stokes shift shows a similar trend with a change in solvent polarity. It varies from 3613 to 7241 cm^{-1} (SDZ), 2868 to 7513 cm^{-1} (SMZ) and 2887 to 7332 cm^{-1} (STZ) from toluene to acetonitrile. Also, Stokes shift varies from 3613 to 9540 cm^{-1} (SDZ), 2868 to 9540 cm^{-1} (SMZ) and 2887 to 9540 cm^{-1} (STZ) from non-polar toluene to polar protic water.

The large shift in the emission spectra and the Stokes shift compared to absorption spectra confirms that the excited state of sulfa drugs was affected to a greater extent by an increase in the polarity of the solvent. This suggests that the dipole moment in the excited state is greater than the dipole moment in the ground state. This is attributed to the intramolecular charge transfer taking place from the electron-donating amino group to the electron-accepting sulfonamide group and pyrimidine ring in all the titled molecules [51]. These results on

significant spectral shifts with solvent polarity indicate the possible use of these molecules in polarity sensing applications.

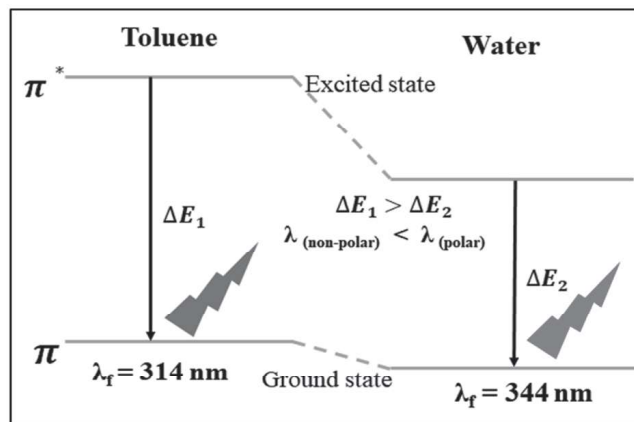


Fig. 4. The $\pi \rightarrow \pi^*$ transition in sulfa drug molecule in Toluene (non-polar) and Water (polar) solvents.

Table 1. Spectral parameters of SDZ, SMZ and STZ molecules in solvents of different polarity.

Solvents	SDZ			SMZ			STZ		
	λ_a (nm)	λ_f (nm)	$\Delta\bar{\nu}$ (cm^{-1})	λ_a (nm)	λ_f (nm)	$\Delta\bar{\nu}$ (cm^{-1})	λ_a (nm)	λ_f (nm)	$\Delta\bar{\nu}$ (cm^{-1})
Hexane	278	302	2858	278	301	2748	278	301	2748
Toluene	282	314	3613	283	308	2868	282	307	2887
Benzene	279	318	4096	276	318	4485	276	318	4485
1,4 Dioxane	279	319	4494	267	304	4558	-	-	-
THF	268	319	5965	269	316	5529	269	317	5628
Ethyl Acetate	-	-	-	-	-	-	268	326	6638
Butyl acetate	267	328	6965	268	330	7010	269	330	6871
Chloroform	-	-	-	-	-	-	266	325	6824
DCM	266	326	6919	266	326	6919	262	319	6819
DCE	-	-	-	-	-	-	266	328	7106
DMF	272	336	7002	272	336	7002	272	339	7266
DMSO	-	-	-	274	345	7510	-	-	-
Acetonitrile	267	331	7241	267	334	7513	267	332	7332
1-Octanol	276	312	4180	276	311	4077	276	315	4485
2-propanol	-	-	-	271	335	7049	270	331	6825
Propanol	269	330	6871	269	332	7054	269	331	6963
Ethanol	269	331	6963	-	-	-	-	-	-
Methanol	267	335	7602	269	337	7501	269	337	7501
Water	259	344	9540	259	344	9540	259	344	9540

THF-Tetrahydrofuran, DCM-Dichloromethane, DCE-Dichloroethane, DMSO-Dimethyl sulfoxide, DMF-Dimethylformamide,

To get a further vision of the solvatochromic behaviour of these sulfa drugs, spectroscopic properties are associated with different solvent polarity parameters. The absorption ($\bar{\nu}_a$ in cm^{-1}), emission ($\bar{\nu}_f$ in cm^{-1}), and Stokes shift ($\Delta\bar{\nu}$ in cm^{-1}) are correlated with bulk solvent polarity parameter (F_{L-M}) at the absorption wavenumber (nearly $R^2=0.30$) shows a poor correlation with F_{L-M} compared to the emission wavenumber (nearly $R^2 = 0.60$) and Stokes shift (nearly $R^2 = 0.62$) in which the correlation is moderate for all the sulfa drugs. The poor and moderate correlation observed in F_{L-M} implies that it doesn't comprehensively account for solvent effects in the mentioned molecules. This could stem from the fact that the F_{L-M} polarity scale overlooks specific solute-solvent interactions such as complex formation, hydrogen bonding effects, charge transfer interactions and others. Therefore, an attempt has been made to correlate spectroscopic properties of titled molecules with E_N^T . The correlation coefficients for E_N^T corresponding to absorption ($\bar{\nu}_a$ in cm^{-1}) are nearly $R^2 = 0.4$ for all sulfa drugs. The corresponding values for fluorescence are nearly $R^2 = 0.63$ for all sulfa drugs. Similarly, $\Delta\bar{\nu}$ has shown correlation coefficients of nearly $R^2 = 0.64$ for all molecules. Here the correlation is almost moderate. This provoked us to correlate the spectroscopic properties with specific set of solvents. Then, the spectroscopic properties are correlated with E_N^T distinctly for solvents belonging to non-alcoholic and alcoholic class. It has been identified that correlation of spectroscopic properties with E_N^T for said class of solvents is reasonably good except in absorption and these plots are shown in Fig. 5 for SDZ (Similar plots for SMZ and STZ are given in Fig.S1 and Fig.S2) with respective correlation coefficients. The reasonably good double linear correlation in emission and Stokes shift indicates that solvent stabilization of excited states is due to a variety of solute-solvent interactions such as hydrogen bonding and dipole-dipole interactions. In protic solvents, increasing polarity stabilizes the molecule through hydrogen bonding. On the other hand, in aprotic solvents, dipole-dipole and dipole-induced dipole forces are assumed to be the predominant interactions.

The reasonably good double linear correlation observed in emission and Stokes shift suggests that the excited state of solutes is stabilised

by various solute-solvent interactions, including hydrogen bonding and dipole-dipole interactions. In solvents of protic nature, increased polarity stabilizes the molecule via hydrogen bonding. Conversely, in solvents of aprotic nature, dipole-dipole and dipole-induced dipole forces are presumed to be the primary interactions.

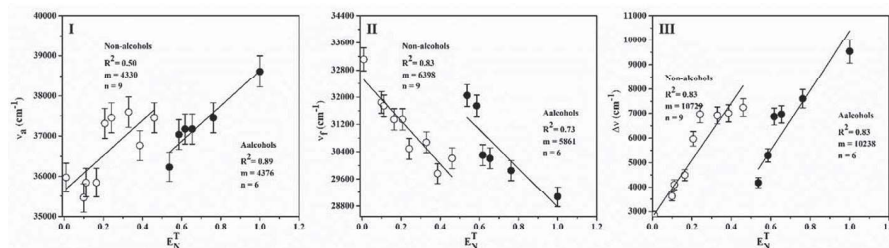


Fig. 5. The plot of (I) $\bar{\nu}_a$ vs E_N^T , (II) $\bar{\nu}_f$ vs E_N^T and (III) $\Delta\bar{\nu}$ vs E_N^T for SDZ molecule.

The correlations are based on ΔF_{L-M} and E_N^T yields solute-solvent interaction mechanisms which are summative of general solute-solvent and specific solute-solvent interaction mechanisms. These methods are unable to identify the individual contribution from either general solute-solvent or specific solute-solvent interaction mechanisms. For this reason, to identify the individual contribution from non-specific dielectric interaction, hydrogen bond donor (HBD) and hydrogen bond acceptor (HBA) ability of solvents, the spectral properties are correlated with solvent polarity parameters proposed by Kamlet and others based on multiple regression [36]. The Kamlet parameters include the hydrogen bond donor ability of a solvent (α), the hydrogen bond acceptor ability of a solvent (β) and non-specific dielectric interaction (π^*). The multiple regression is carried out and correlation data is presented in Eqs. (21), (22) and (23).

SDZ

$$\begin{aligned}
 \bar{\nu}_a \text{ (cm}^{-1}\text{)} &= 35754 + 610 \alpha + 304 \beta + 1390 \pi^* & R^2 &= 0.30 \\
 \bar{\nu}_f \text{ (cm}^{-1}\text{)} &= 33105 - 264 \alpha - 578 \beta - 3265 \pi^* & R^2 &= 0.84 \\
 \Delta\bar{\nu} \text{ (cm}^{-1}\text{)} &= 2648 + 875 \alpha + 883 \beta + 4656 \pi^* & R^2 &= 0.77
 \end{aligned}
 \tag{21}$$

SMZ

$$\begin{array}{l}
 \bar{\nu}_a \text{ (cm}^{-1}\text{)} = 336153 + 590 \alpha - 136 \beta + 1131 \pi^* \quad R^2 = 0.54 \\
 \bar{\nu}_f \text{ (cm}^{-1}\text{)} = 33345 - 581 \alpha - 1465 \beta - 3109 \pi^* \quad R^2 = 0.82 \\
 \Delta\bar{\nu} \text{ (cm}^{-1}\text{)} = 2607 - 1172 \alpha + 1328 \beta + 4240 \pi^* \quad R^2 = 0.79
 \end{array}
 \quad \left. \vphantom{\begin{array}{l} \\ \\ \end{array}} \right\} (22)$$

STZ

$$\begin{array}{l}
 \bar{\nu}_a \text{ (cm}^{-1}\text{)} = 36006 - 427 \alpha - 238 \beta + 1795 \pi^* \quad R^2 = 0.64 \\
 \bar{\nu}_f \text{ (cm}^{-1}\text{)} = 33215 - 405 \alpha - 1434 \beta - 2886 \pi^* \quad R^2 = 0.84 \\
 \Delta\bar{\nu} \text{ (cm}^{-1}\text{)} = 2790 + 832 \alpha + 1196 \beta + 4681 \pi^* \quad R^2 = 0.78
 \end{array}
 \quad \left. \vphantom{\begin{array}{l} \\ \\ \end{array}} \right\} (23)$$

Based on the equations provided earlier, it is confirmed that the general dielectric interaction (π^*) of solvents has a major influence on sulfa drugs. However, the contributions from HBD and HBA cannot be neglected. From multiple linear regression data $\bar{\nu}_a$, $\bar{\nu}_f$ and $\Delta\bar{\nu}$, HBA influence is more than HBD in all these molecules. This might be due to two electron-withdrawing sulfonyl oxygen atoms present in these molecules.

From Kamlet's analysis, it is hard to identify the individual contributions due to the polarizability and dipolarity of solvents. Hence, in order to determine the distinct influences of solvent polarity and dipolarity, the spectral properties are correlated with the solvent polarity parameter scale introduced by Catalan and colleagues using multiple regression analysis [37]. The multiple regression is carried out based on the Catalan scale and correlation data is presented in Eqs. (24), (25) and (26).

SDZ

$$\begin{array}{l}
 \bar{\nu}_a \text{ (cm}^{-1}\text{)} = 39338 - 218 SA - 526 SB - 4997 SP - 2003 SdP \quad R^2 = 0.86 \\
 \bar{\nu}_f \text{ (cm}^{-1}\text{)} = 32674 + 105 SA + 959 SB - 73 SP - 3632 SdP \quad R^2 = 0.93 \\
 \Delta\bar{\nu} \text{ (cm}^{-1}\text{)} = 6663 + 113 SA - 1485 SB - 4923 SP + 5636 SdP \quad R^2 = 0.93
 \end{array}
 \quad \left. \vphantom{\begin{array}{l} \\ \\ \end{array}} \right\} (24)$$

SMZ

$$\begin{array}{ll}
 \bar{\nu}_a \text{ (cm}^{-1}\text{)} = 36071 + 808 \text{ SA} - 208 \text{ SB} - 1785 \text{ SP} + 1114 \text{ SdP} & R^2 = 0.63 \\
 \bar{\nu}_f \text{ (cm}^{-1}\text{)} = 31329 - 168 \text{ SA} + 332 \text{ SB} + 2629 \text{ SP} - 3917 \text{ SdP} & R^2 = 0.93 \\
 \Delta\bar{\nu} \text{ (cm}^{-1}\text{)} = 4741 + 976 \text{ SA} - 541 \text{ SB} - 2451 \text{ SP} + 5032 \text{ SdP} & R^2 = 0.91
 \end{array} \quad (25)$$

STZ

$$\begin{array}{ll}
 \bar{\nu}_a \text{ (cm}^{-1}\text{)} = 37263 - 185 \text{ SA} - 954 \text{ SB} - 1509 \text{ SP} + 2086 \text{ SdP} & R^2 = 0.73 \\
 \bar{\nu}_f \text{ (cm}^{-1}\text{)} = 32455 - 317 \text{ SA} - 168 \text{ SB} + 713 \text{ SP} - 3271 \text{ SdP} & R^2 = 0.92 \\
 \Delta\bar{\nu} \text{ (cm}^{-1}\text{)} = 4807 + 299 \text{ SA} - 785 \text{ SB} - 2222 \text{ SP} + 5358 \text{ SdP} & R^2 = 0.90
 \end{array} \quad (26)$$

The above results imply that the correlation is relatively good compared to Kamlet's regression. The correlation data based on emission and Stokes shift indicates that the solvent dipolarity influence is more compared to solvent polarity, SA and SB. The solvent basicity influences more than the solvent acidity. The results obtained by Kamlet's and Catalan are in good agreement with each other.

4.2. Preferential Solvation Study

Preferential solvation studies have been carried out using the THF-Water binary mixture. The absorption and fluorescence spectra of titled molecules were recorded in the THF-Water binary mixture and are given in Fig.6 and Fig.7 respectively.

The absorption spectra of titled molecules in the THF-Water mixture suffer a blue shift from 269nm to 259nm on increasing the composition of water as shown in Fig. 6 with respect to pure THF. Fig. 8 represents the preferential behaviour of sulfa drugs in the ground state and it shows the large deviation from the ideal case. This indicates that solute molecules are preferentially solvated either by THF or Water. To find whether the said molecules are preferentially solvated by THF or water, the parameters δ_{12} and K_{sp} are estimated. These values are given in Table 2. From Table 2, for ground state $\delta_{12} < 0$ and $K_{sp} < 1$. This confirms that the titled molecules are solvated by first solvent i.e. THF. The hydroxylic component ROH% value in the ground state for all molecules was estimated using Eqn. (9) and is found to be nearly

10% in the THF-Water mixture. This suggests that only 10 percent of H₂O molecules have entered the solvation shell and are linked to sulfa drugs. This also suggests a greater abundance of THF molecules in the solvation shell, establishing effective interactions with the titled molecules. Therefore, the large deviation of experimental data from ideal case indicates that titled molecules are preferentially solvated by THF in the ground state.

However, the fluorescence spectra have not shown any systematic variation of fluorescence maxima on increasing the composition of water (Fig. 7). Fig. 9 represents the preferential behaviour of sulfa drugs in the excited state and it shows the large deviation from the ideal case. Fluorescence spectra have shown a blue shift up to $X_2 = 0.94$ in all the molecules, and for $X_2 > 0.94$ they show a red shift with respect to THF. It means the $\bar{\nu}_{12}(\text{cm}^{-1})$ value increases up to $X_2 = 0.94$ and for $X_2 > 0.94$ its value decreases abruptly. The fluorescence spectra arise from the ICT state brought by the polarity of the complex formed among solvent molecules (THF: Water). The shift in fluorescence spectra for all molecules is the result of preference for intermolecular hydrogen bonding between solutes and THF:Water complex. This is called synergistic effect. The synergistic effect generally occurs in a binary mixture, where one solvent serves as a hydrogen bond contributor and the other serves as a hydrogen bond acceptor, both forming an association with each other, resulting in a more polar H-bonded complex [18]. In THF -Water binary mixture, water acts as a hydrogen bond donor ($\alpha = 1.17$, $\beta = 0.18$) and THF acts as a hydrogen bond acceptor ($\alpha = 0.00$, $\beta = 0.55$), leading to the formation of more polar H-bonded complex. The solute molecules are preferentially solvated by these H-bonded complexes more than any individual solvent used in the solvent mixture. In this situation, due to the influence of the synergistic effect it is difficult to evaluate parameters of solvation according to the local excess model. These results in the THF-Water binary solvent mixture indicate that the titled molecules could be used to detect aqueous content in organic solvents and other chemicals [18].

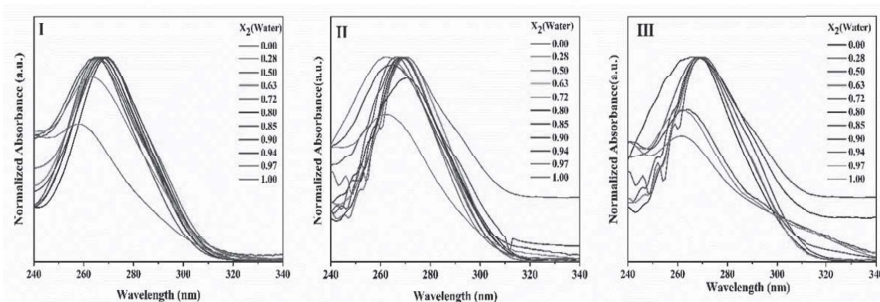


Fig. 6. Normalized absorption spectra of (I) SDZ, (II) SMZ and (III) STZ in THF-Water mixture.

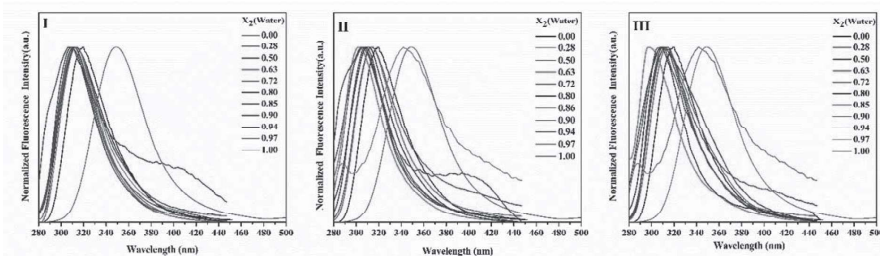


Fig. 7. Normalized fluorescence spectra for (I) SDZ, (II) SMZ and (III) STZ in THF-Water mixture.

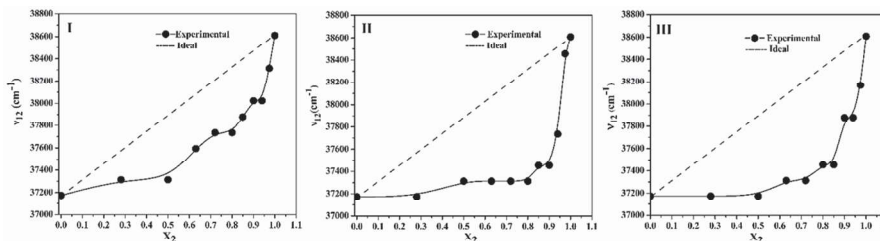


Fig. 8. Plot of $\bar{\nu}_{12}$ vs X_2 in ground state for (I) SDZ, (II) SMZ and (III) STZ in THF-Water.

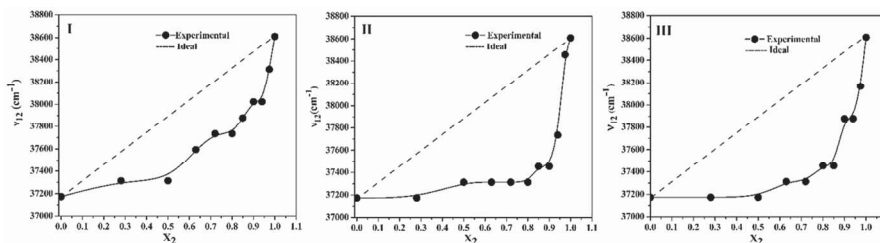


Fig. 9. Plot of $\bar{\nu}_{12}$ vs X_2 in excited state for (I) SDZ, (II) SMZ and (III) STZ in THF-Water.

Table 2(a). Preferential solvation parameters for SDZ molecule in THF-Water.

X_2	$\bar{v}_{12}(\text{cm}^{-1})$		X_2^L		δ_{12}		Ksp	
	GS	ES	GS	ES	GS	ES	GS	ES
0.00	37174	31347	0.00	0.00	0.00	-	-	-
0.28	37174	31948	0.00	-0.26	-0.28	-	0	-
0.50	37313	32258	0.09	-0.39	-0.40	-	0.10	-
0.63	37313	32051	0.09	-0.30	-0.53	-	0.06	-
0.72	37453	32051	0.19	-0.30	-0.52	-	0.09	-
0.80	37453	31847	0.19	-0.21	-0.60	-	0.05	-
0.85	37735	32154	0.39	-0.35	-0.45	-	0.10	-
0.90	37735	32051	0.39	-0.30	-0.50	-	0.06	-
0.94	37735	32362	0.39	-0.44	-0.54	-	0.03	-
0.97	38022	31055	0.59	0.12	-0.38	-	0.03	-
1.00	38610	29069	1.00	1.00	0.00	-	-	-

Table 2(b). Preferential solvation parameters for SMZ molecule in THF-Water.

X_2	$\bar{v}_{12}(\text{cm}^{-1})$		X_2^L		δ_{12}		Ksp	
	GS	ES	GS	ES	GS	ES	GS	ES
0.00	37174	31645	0.00	0.00	0.00	-	-	-
0.28	37174	31847	0.00	-0.07	-0.28	-	0.00	-
0.50	37313	32362	0.09	-0.27	-0.40	-	0.10	-
0.63	37313	33003	0.09	-0.52	-0.53	-	0.06	-
0.72	37313	32573	0.09	-0.36	-0.62	-	0.04	-
0.80	37313	32154	0.09	-0.19	-0.70	-	0.02	-
0.85	37453	32679	0.19	-0.40	-0.65	-	0.04	-
0.90	37453	31847	0.19	-0.07	-0.70	-	0.02	-
0.94	37735	32573	0.39	-0.36	-0.54	-	0.03	-
0.97	38461	29239	0.89	0.93	-0.07	-	0.22	-
1.00	38610	29069	1.00	1.00	0.00	-	-	-

Table 2(c). Preferential solvation parameters for STZ molecule in THF-Water.

χ_2	$\bar{\nu}_{12}(\text{cm}^{-1})$		X_2^L		δ_{12}		Ksp	
	GS	ES	GS	ES	GS	ES	GS	ES
0.00	37174	31545	0.00	0.00	0.00	-	-	-
0.28	37174	32051	0.00	-0.20	-0.28	-	0.00	-
0.50	37174	32154	0.00	-0.24	-0.50	-	0.00	-
0.63	37313	33003	0.09	-0.58	-0.53	-	0.06	-
0.72	37313	31948	0.09	-0.16	-0.62	-	0.04	-
0.80	37453	32467	0.19	-0.37	-0.60	-	0.05	-
0.85	37453	32154	0.19	-0.24	-0.65	-	0.04	-
0.90	37878	32258	0.49	-0.28	-0.40	-	0.10	-
0.94	37878	32258	0.49	-0.28	-0.44	-	0.05	-
0.97	38167	29498	0.69	0.82	-0.28	-	0.05	-
1.00	38610	29069	1.00	1.00	0.00	-	-	-

4.3. Ground and Excited State Dipole Moments based on Solvatochromism in Neat Solvents.

The ground state and excited state dipole moment of all the molecules in the gaseous phase were obtained by quantum chemical computations with Gaussian 09 software, utilizing the B3LYP level of theory and 6-311+ G(d, p) basis set. These values are given in Table 3. The titled molecules have large ground state dipole moments varying from 6.52D – 7.56D. These high values of ground state dipole moments are attributed to asymmetric geometry and polar nature of these molecules. The quantum chemical calculations indicate that the dipole moment in the excited state of all the titled molecules is greater than its ground state counterpart. The magnitude and direction of dipole moment vector for optimized SDZ molecule for both ground and excited states are depicted in Fig.10. Fig.10 also suggests dipole moment in the excited state is greater than its ground state partner. Similar results are observed for other molecules.

Methods	SDZ			SMZ			STZ		
	$\mu_g = 6.52$	$a = 4.04$	$\mu_g = 6.33$	$\mu_g = 6.33$	$a = 4.21$	$\mu_g = 7.56$	$a = 4.36$		
	μ_e	$\Delta\mu$	μ_e	μ_e	$\Delta\mu$	μ_e	$\Delta\mu$		
Computational method	8.6	2.08	8.42	8.42	2.09	10.06	2.5		
L-M	14.61	8.09	14.92	14.92	8.59	16.99	11.43		
B-K	11.29	4.77	11.4	11.4	5.07	12.88	5.32		
K-C-V	7.5	0.98	7.34	7.34	1.01	8.16	0.6		
Non-alcohols	11.49	4.97	11.28	11.28	4.95	12.99	5.43		
Alcohols	11.63	5.11	10.08	10.08	3.75	11.47	3.91		

Table 3. Theoretically estimated dipole moments in ground state (μ_g) (D), values of Onsager radius (a) (Å), dipole moment in excited state (μ_e) (D) and change in dipole moment ($\Delta\mu$) (D) obtained using various models for sulfa drugs.

L-M: Lippert-Mataga, B-K: Bakhshiev, K-C-V: Kawski-Chamma-Viallet's

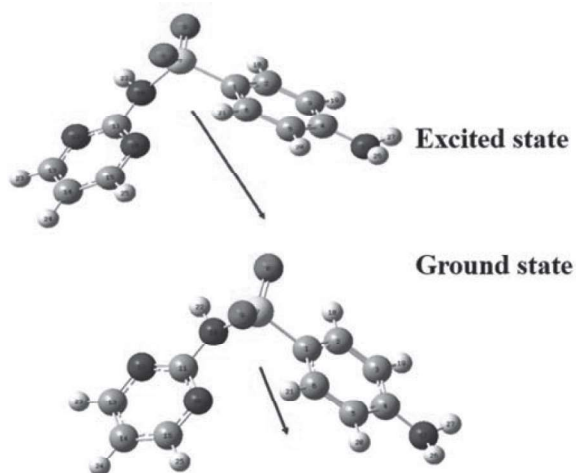


Fig. 10. Optimised structure of SDZ molecule with its vector notation in ground state and excited state.

The solvatochromic data obtained in neat solvents for titled molecules presented in Table 1 has been used in this section. The excited state dipole moment of all the molecules was determined by Lippert-Mataga, Bakhshiev's, Kawski-Chamma-Viallet and Reichardt's correlation using Eqs. (10), (11), (12) and (16) and corresponding linear correlation plots for all the molecules are shown in Fig.11 for SDZ. Similar plots for SMZ and STZ are presented in Fig. S3 and Fig. S4 of supplementary material. The good correlation coefficient values obtained for selected data points (For Fig. 11.I - Benzene, 1,4 Dioxane, THF, DMF, ACN, Propanol, Ethanol. Fig. 11.II - Benzene, 1,4 Dioxane, THF, DCE, DMF, ACN and Propanol. Fig 11.III - 1,4 Dioxane, Toluene, DCE, Butanol. Fig. 11.IV - Hexane, Toluene, Benzene, 1,4 Dioxane, Butyl Acetate, DMF, ACN, Octanol, Butanol, Methanol and Water) are ranging from 0.96 to 0.99. in all these plots (Fig.12). By using slopes of these plots and dipole moment obtained for ground state from quantum chemical calculations, the dipole moments for the excited state are calculated. The double linear correlation of $\Delta\bar{\nu}$ vs E_N^T for selected data points in alcohols and non-alcohols motivated us to estimate excited state dipole moment distinctly for solvents belongs to the class of alcohols and non-alcohols. These values are also presented in Table 3. As observed from Table 3, the excited state dipole moment is greater than its counterpart in the ground state for

all the molecules. This is in good agreement with quantum chemical calculations. The rise in value of excited state dipole moment could be due to charge density redistribution between the electronic states, intermolecular bonding between solute-solvent, ICT and the geometrical variations occurs among different electronic states. The ICT in these molecules occurs from the -NH_2 to the pyrimidine ring as evidenced from TD-DFT calculations and is depicted in Fig.12 for SDZ molecule. The ICT in these molecules is also attributed to the existence of different resonance structures of the titled molecules as shown in Fig.13.

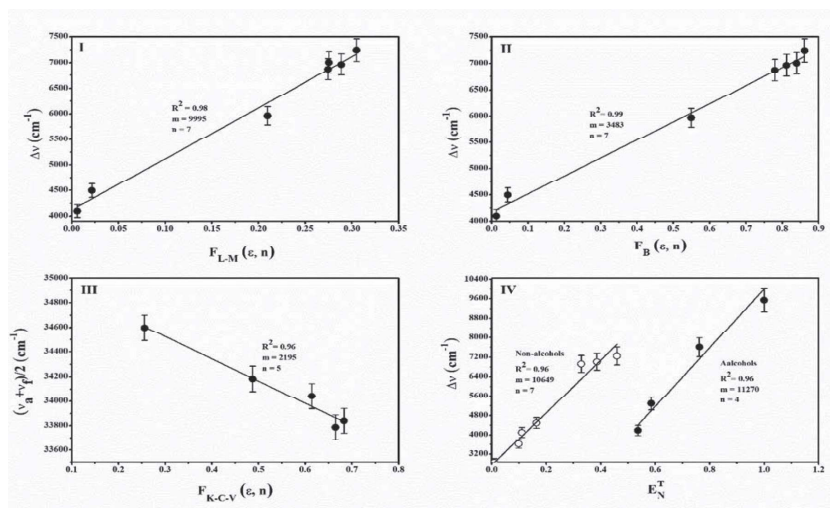


Fig. 11. Solvatochromic linear correlation of (I) Lippert-Mataga, (II) Bakhshiev's, (III) Kawski-Chamma-Violet and (IV) Reichardt method for SDZ molecule.

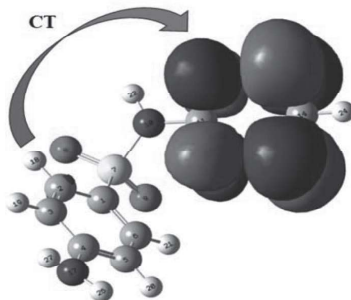


Fig. 12. The LUMO diagram of SDZ molecule from TD-DFT calculation indicating ICT takes place from -NH_2 group to the pyrimidine ring.

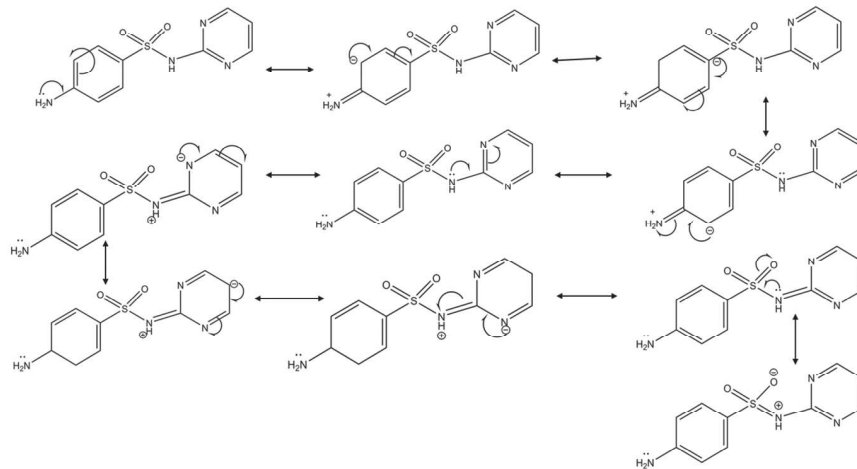


Fig. 13 (a). Resonance structures of SDZ molecule.

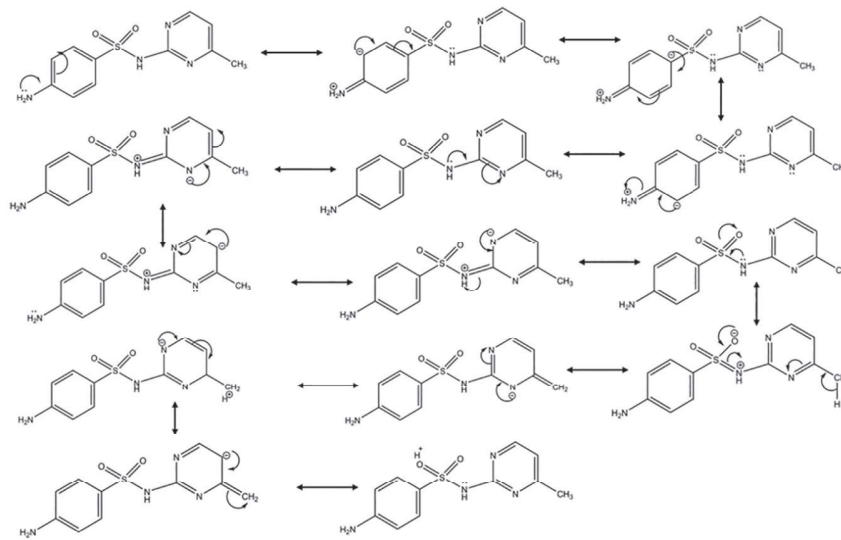


Fig. 13 (b). Resonance structures of SMZ molecule.

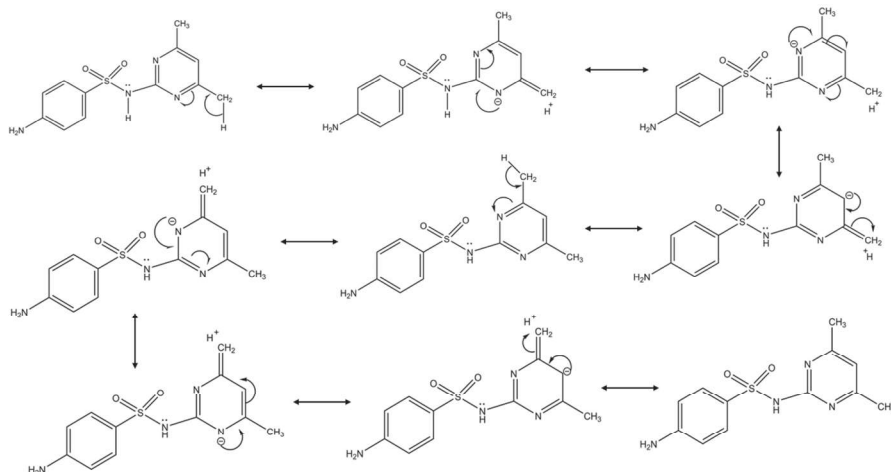


Fig. 13 (c). Resonance structures of STZ molecule.

The excited dipole moments obtained by the Lippert-Mataga correlation method are higher as compared with other methods. This is because the polarizability of molecules is not considered in this method while treating solute-solvent interactions. As observed from Table 3, the μ_e values calculated from the Kawski-Chamma-Viallet method are smaller compared to the values calculated from other methods and are comparable to values obtained from the calculations based on the quantum chemistry. The variations in calculated excited state dipole moment values across different methods may arise from the disparate assumptions inherent in each method [27,28]. From Table 3, it is observed that the change in dipole moment estimated using quantum chemical calculation is more compared to the experimental method (Kawski-Chamma Viallet). This happens generally because the quantum chemical calculations overestimate the physical parameters in gaseous phase. The difference in dipole moment ($\Delta\mu$) values calculated from different solvatochromic models are also given in Table 3. For all sulfa drugs, the significance difference in $\Delta\mu$ values was observed among all the solvatochromic models. The lowest values are obtained from Kawski-Chamma-Viallet model, whereas the maximum values are obtained for Lippert-Mataga model. The noticeable difference between $\Delta\mu$ values is comprehended in terms of polarizability effect. As discussed above, the polarizability term was neglected in Lippert-Mataga model whereas the Bakhshiev's model

assumed the polarizability factor $2\alpha/a^3 = 1$. Hence, the noticeable difference in $\Delta\mu$ values calculated using different theoretical models are evidently indicate that the solute polarizability affects the $\Delta\mu$ of the titled molecules upon excitation [53].

To study solute polarizability influence on dipole moments in excited state and difference in dipole moments, the equation (18) according to Bilot-Kawski was used. The polarizability dependent polarity function $F_{B-K}(\epsilon, n)$ for different values of $2\alpha/a^3$ ($0 \leq 2\alpha/a^3 \leq 1$) is calculated from Eqn (20) and is given in Table S1 of supplementary material. The excited state dipole moments and difference in dipole moments calculated for different value of $2\alpha/a^3$ ($0 \leq 2\alpha/a^3 \leq 1$) are given in Table 4. As seen from Table 4, with increase in $2\alpha/a^3$ the dipole moment in excited state and change in dipole moment values decreases continuously. The difference in dipole moment values calculated for two values of $2\alpha/a^3 = 0$ and $2\alpha/a^3 = 1$ differ by 25% for all the titled molecules, confirming that the dipole moment in excited state and difference in dipole moment was affected by polarizability of solute molecule. These results indicate the importance of consideration of polarizability of solute molecule in estimating its excited state dipole moment.

Molecule	$(0 \leq 2\alpha/a^3 \leq 1)$										
	0	0.1	0.2	0.3	0.4	0.5	0.6	0.7	0.8	0.9	1
	$\mu_{eB-K}(D)$ as a functions of $2\alpha/a^3$										
SDZ	14.76	14.4	14.06	13.72	13.37	13.04	12.7	12.36	12.03	11.69	11.36
SMZ	14.92	14.56	14.2	13.84	13.48	13.13	12.77	12.42	12.07	11.72	11.37
STZ	18.98	18.5	18.03	17.56	17.09	16.62	16.16	15.7	15.23	14.77	14.31
	$\Delta\mu_{B-K}(D)$ as a functions of $2\alpha/a^3$										
SDZ	8.23	7.88	7.54	7.2	6.85	6.52	6.18	5.84	5.51	5.17	4.84
SMZ	8.59	8.23	7.87	7.51	7.15	6.8	6.44	6.09	5.74	5.39	5.04
STZ	11.42	10.94	10.47	10	9.53	9.06	8.6	8.14	7.67	7.21	6.75

Table 4. The values of state dipole moment in excited ($\mu_{eB-K}(D)$) and change in dipole moment ($\Delta\mu_{B-K}(D)$) calculated from Bilot-Kawski method for SDZ, SMZ and STZ as a function of $0 \leq 2\alpha/a^3 \leq 1$.

5. Conclusion

The examination of solvatochromism in sulfa drug molecules of medicinal significance revealed a hypsochromic (blue) shift in the UV-Visible absorption spectra and a bathochromic (red) shift in fluorescence spectra in response to changes in solvent polarity. The observed significant spectral shifts in relation to solvent polarity suggest the potential use of these molecules as probes for polarity sensing. Employing the regression approaches proposed by Kamlet-Taft and Catalan, it was determined that non-specific solute-solvent interactions predominantly influence all drug molecules, with minor contributions from solute-solvent specific interactions. The preferential solvation study indicated that the investigated drugs are solvated by extremely polar hydrogen bonded complex formed through solvent-solvent interaction between THF and water. The results affirm the suitability of the studied drug molecules for detecting aqueous content in organic solvents or chemicals. Furthermore, the estimated excited state dipole moment using various methods was found to be higher than its ground state counterpart. The dependence of the excited state dipole moment and the change in dipole moment on polarizability underlines the importance of considering solute polarizability in various solvatochromic models. To the utmost extent understanding, this study represents the preliminary comprehensive investigation into solvatochromism, solvation, and the evaluation of dipole moments of sulfa drug molecules. The promising results from this study suggest potential applications of the investigated drug molecules in areas such as polarity sensing and moisture detection, in addition to their established biomedical and pharmaceutical uses.

Acknowledgment

The author Vibha thanks Govt. of Karnataka for awarding monthly fellowship through Backward Classes Welfare Department to pursue Ph.D. at the Dept. of Physics, Vijayanagara Sri Krishnadevaraya University, Ballari, Karnataka, India.

Credit authorship contribution statement:

Vibha: Investigation, Visualisation, Validation, Data curation, Writing-Original draft. **Prachalith N.C:** Methodology, Resources,

Data curation, editing,. Validation, **Suresh Kumar H M:** Data curation, Visualization, Project administration., **Ravikantha M.N:** Resources, Data curation, software **Annoji Reddy R:** Validation, Visualisation, **Thipperudrappa J:** Roles/Writing - original draft and Writing - review & editing, Supervision, Project administration.

Conflict of Interest:

We the authors of this manuscript declare that there is no conflict of interest concerning this work.

References:

- [1] Monnais, L. (2009). From Colonial Medicines to Global Pharmaceuticals? The Introduction of Sulfa Drugs in French Vietnam. *East Asian Science, Technology and Society: An International Journal*, 3, 257-285. doi:10.1007/s12280-009-9083-8.
- [2] Ovung, A., & Bhattacharyya, J. (2021). Sulfonamide drugs: Structure, antibacterial property, toxicity, and biophysical interactions. *Biophysical reviews*, 13(2), 259-272. doi: 10.1007/s12551-021-00795-9.
- [3] Ghorab, M. M., M. Soliman, A., El-Sayyad, G. S., Abdel-Kader, M. S., & El-Batal, A. I. (2023). Synthesis, Antimicrobial, and Antibiofilm Activities of Some Novel 7-Methoxyquinoline Derivatives Bearing Sulfonamide Moiety against Urinary Tract Infection-Causing Pathogenic Microbes. *International Journal of Molecular Sciences*, 24(10), 8933. doi: 10.3390/ijms24108933.
- [4] Pryles, C. V. (1970). The Use of Sulfonamides in Urinary Tract Infection. *Medical Clinics of North America*, 54(5), 1077-1080. doi: 10.1016/s0025-7125(16)32578-0.
- [5] Baran, W., Adamek, E., Ziemiańska, J., & Sobczak, A. (2011). Effects of the presence of sulfonamides in the environment and their influence on human health. *Journal of hazardous materials*, 196, 1-15. doi: 10.1016/j.jhazmat.2011.08.082.
- [6] Ali, H., & Goswami, D. (2023). Demonstration of solute-specific synergism in binary solvents. *Journal of Fluorescence*, 1-11. doi: 10.1007/s10895-022-03141-8.
- [7] Awaisheh, S. S., Khalifeh, M. S., Rahahleh, R. J., Ja'far, M., & Algroom, R. M. (2019). Sulfamethazine contamination level and exposure assessment in domestic and imported poultry

- meats in Jordan. *Veterinary World*, 12(12), 1992. doi: 10.14202/vetworld.2019.1992-1997.
- [8] Venning, D. R., Mousa, J. J., Lukasiewicz, R. J., & Winefordner, J. D. (1972). Influence of solvent upon the phosphorescence characteristics of several sulfonamides at 77. deg. K. *Analytical Chemistry*, 44(14), 2387-2389. doi: 10.1021/ac60322a044.
- [9] Sterling, J. M., & Haney, W. G. (1974). Spectrophotofluorometric analysis of procainamide and sulfadiazine in presence of primary aliphatic amines based on reaction with fluorescamine. *Journal of Pharmaceutical Sciences*, 63(9), 1448-1450. doi: 10.1002/jps.2600630925.
- [10] Pang, G. F., Cao, Y. Z., Fan, C. L., Zhang, J. J., Li, X. M., Li, Z. Y., & Jia, G. Q. (2003). Liquid chromatography–fluorescence detection for simultaneous analysis of sulfonamide residues in honey. *Analytical and bioanalytical chemistry*, 376(4), 534-541. doi: 10.1007/s00216-003-1883-4
- [11] Bitas, D., Kabir, A., Locatelli, M., & Samanidou, V. (2018). Food sample preparation for the determination of sulfonamides by high-performance liquid chromatography: State-of-the-art. *Separations*, 5(2), 31.
- [12] Naresh, K. (2014). Applications of fluorescence spectroscopy. *J. Chem. Pharm. Sci*, 974, 2115.
- [13] Shahzad, A., Köhler, G., Knapp, M., Gaubitzer, E., Puchinger, M., & Edetsberger, M. (2009). Emerging applications of fluorescence spectroscopy in medical microbiology field. *Journal of Translational Medicine*, 7, 1-6. doi: 10.1186/1479-5876-7-99.
- [14] Bose, A., Thomas, I., & Abraham, E. (2018). Fluorescence spectroscopy and its applications: A Review. *Int. J. Adv. Pharm. Res*, 8(1), 1-8. doi: 10.7439/ijapa
- [15] Andersen, C. M., & Mortensen, G. (2008). Fluorescence spectroscopy: A rapid tool for analyzing dairy products. *Journal of agricultural and food chemistry*, 56(3), 720-729. doi: https://doi.org/10.1021/jf072025o.
- [16] Shkoor, M., Mehanna, H., Shabana, A., Farhat, T., & Bani-Yaseen, A. D. (2020). Experimental and DFT/TD-DFT computational investigations of the solvent effect on the spectral properties of nitro substituted pyridino [3, 4-c] coumarins. *Journal of Molecular Liquids*, 313, 113509. doi: 10.1016/j.molliq.2020.113509.

- [17] Raghavendra, U. P., Basanagouda, M., Melavanki, R. M., Fattepur, R. H., & Thipperudrappa, J. (2015). Solvatochromic studies of biologically active iodinated 4-aryloxymethyl coumarins and estimation of dipole moments. *Journal of Molecular Liquids*, 202, 9-16. doi: 10.1016/j.molliq.2014.12.003.
- [18] Husain, S., Pandey, N., Fatma, N., Pant, S., & Mehata, M. S. (2022). Spectral characteristics of 3, 5-diaminobenzoic acid in pure and mixed solvents: Experimental and theoretical study. *Journal of Molecular Liquids*, 368, 120783. doi: 10.1016/j.molliq.2022.120783.
- [19] Deepa, H. R., Thipperudrappa, J., Fattepur, R. H., & Kumar, H. S. (2013). Solvatochromic shift studies in LD-425 and LD-423: Estimation of ground and excited state dipole moments. *Journal of Molecular Liquids*, 181, 82-88. doi: 10.1016/j.molliq.2013.02.016.
- [20] Patil, M. K., Kotresh, M. G., Tilakraj, T. S., & Inamdar, S. R. (2022). Solvatochromism and ZINDO-IEFPCM solvation study on NHS ester activated AF514 and AF532 dyes: Evaluation of the dipole moments. *European Journal of Chemistry*, 13(1), 8-19. doi: 10.5155/eurjchem.13.1.8-19.2123.
- [21] Melavanki, R., Sharma, K., Muttannavar, V. T., Kusanur, R., Katagi, K., Patra, S. M., ... & Koppal, V. V. (2021). Quantum chemical computations, fluorescence spectral features and molecular docking of two biologically active heterocyclic class of compounds. *Journal of Photochemistry and Photobiology A: Chemistry*, 404, 112956. doi: 10.1016/j.jphotochem.2020.112956.
- [22] Patil, M. K., Kotresh, M. G., & Inamdar, S. R. (2019). A combined solvatochromic shift and TDDFT study probing solute-solvent interactions of blue fluorescent Alexa Fluor 350 dye: Evaluation of ground and excited state dipole moments. *Spectrochimica Acta Part A: Molecular and Biomolecular Spectroscopy*, 215, 142-152. doi: 10.1016/j.saa.2019.02.022.
- [23] Matiadis, D., Nowak, K. E., Alexandratou, E., Hatzidimitriou, A., Sagnou, M., & Papadakis, R. (2021). Synthesis and (fluoro) solvatochromism of two 3-styryl-2-pyrazoline derivatives bearing benzoic acid moiety: A spectral, crystallographic and computational study. *Journal of Molecular Liquids*, 331, 115737. doi: 10.1016/j.molliq.2021.115737.
- [24] Lokshin, V., Sigalov, M., Larina, N., & Khodorkovsky, V. (2021). Dipole moments of conjugated donor-acceptor substituted

- systems: calculations vs. experiments. *RSC advances*, 11(2), 934-945. doi: 10.1039/d0ra10182f.
- [25] Homocianu, M., & Airinei, A. (2015). Investigations of absorption and emission spectral data in mixed liquid media. A short review of recent literature. *Journal of Molecular Liquids*, 209, 549-556. doi: 10.1016/j.molliq.2015.06.042.
- [26] Castro, G. T., Filippa, M. A., Peralta, C. M., Davin, M. V., Almandoz, M. C., & Gasull, E. I. (2018). Solubility and preferential solvation of piroxicam in neat solvents and binary systems. *Zeitschrift für Physikalische Chemie*, 232(2), 257-280. doi: 10.1515/zpch-2017-0946.
- [27] Bhagwat, A. A., & Sekar, N. (2019). Fluorescent 7-substituted coumarin dyes: solvatochromism and NLO studies. *Journal of Fluorescence*, 29, 121-135. doi: 10.1007/s10895-018-2316-2.
- [28] Mohan, M., Pangannaya, S., Satyanarayan, M. N., & Trivedi, D. R. (2018). Photophysical and electrochemical properties of organic molecules: Solvatochromic effect and DFT studies. *Optical Materials*, 77, 211-220. doi: 10.1016/j.optmat.2018.01.031.
- [29] Mataga, N., Kaifu, Y., & Koizumi, M. (1956). Solvent effects upon fluorescence spectra and the dipole moments of excited molecules. *Bulletin of the Chemical Society of Japan*, 29(4), 465-470. doi: 10.1246/bcsj.29.465.
- [30] Govindasamy, P., & Gunasekaran, S. (2015). Quantum mechanical calculations and spectroscopic (FT-IR, FT-Raman and UV) investigations, molecular orbital, NLO, NBO, NLMO and MESP analysis of 4-[5-(4-methylphenyl)-3-(trifluoromethyl)-1H-pyrazol-1-yl] benzene-1-sulfonamide. *Journal of Molecular Structure*, 1081, 96-109. doi: 10.1016/j.molstruc.2014.10.011.
- [31] Bilot, L., & Kawski, A. (1963). Der Einfluß des Lösungsmittels auf die Elektronenspektren lumineszierender Moleküle. *Zeitschrift für Naturforschung A*, 18(1), 10-15. doi: 10.1515/zna-1963-0103.
- [32] Subramanian, M. K., Anbarasan, P. M., & Manimegalai, S. (2009). DFT simulations and vibrational analysis of FT-IR and FT-Raman spectra of 2, 4-diamino-6-hydroxypyrimidine. *Spectrochimica Acta Part A: Molecular and Biomolecular Spectroscopy*, 73(4), 642-649. doi: 10.1016/j.saa.2009.03.006.
- [33] Kawski, A. (2002). On the estimation of excited-state dipole moments from solvatochromic shifts of absorption and

- fluorescence spectra. *Zeitschrift für Naturforschung A*, 57(5), 255-262. doi: 10.1515/zna-2002-0509.
- [34] Kawski, A., Kukliński, B., & Bojarski, P. (2006). Excited state dipole moments of N, N-dimethylaniline from thermochromic effect on electronic absorption and fluorescence spectra. *Chemical physics*, 320(2-3), 188-192. doi: 10.1016/j.chemphys.2005.07.007.
- [35] Reichardt, C. (1994). Solvatochromic dyes as solvent polarity indicators. *Chemical reviews*, 94(8), 2319-2358. doi: 10.1021/cr00032a005.
- [36] Taft, R. W., Abboud, J. L. M., & Kamlet, M. J. (1984). Linear solvation energy relationships. 28. An analysis of Swain's solvent "acidity" and "basicity" scales. *The Journal of Organic Chemistry*, 49(11), 2001-2005. doi: 10.1021/jo00185a034.
- [37] Catalán, J. (2009). Toward a generalized treatment of the solvent effect based on four empirical scales: dipolarity (SdP, a new scale), polarizability (SP), acidity (SA), and basicity (SB) of the medium. *The Journal of Physical Chemistry B*, 113(17), 5951-5960. doi: 10.1021/jp8095727.
- [38] Kamlet, M. J., Abboud, J. L. M., Abraham, M. H., & Taft, R. W. (1983). Linear solvation energy relationships. 23. A comprehensive collection of the solvatochromic parameters, π^* , α , and β , and some methods for simplifying the generalized solvatochromic equation. *The Journal of Organic Chemistry*, 48(17), 2877-2887. doi:10.1021/jo00165a018.
- [39] Laha, A. K., Das, P. K., & Bagchi, S. (2002). Study of preferential solvation in mixed binary solvent as a function of solvent composition and temperature by UV-Vis spectroscopic method. *The Journal of Physical Chemistry A*, 106(13), 3230-3234. doi: 10.1021/jp0121116.
- [40] Catalán, J., Díaz, C., & Garcia-Blanco, F. (2000). Characterization of binary solvent mixtures. *The Journal of Organic Chemistry*, 65(26), 9226-9229. doi: 10.1021/jo001008u.
- [41] Sandri, C., de Melo, C. E., Giusti, L. A., Rezende, M. C., & Machado, V. G. (2021). Preferential solvation index as a tool in the analysis of the behavior of solvatochromic probes in binary solvent mixtures. *Journal of Molecular Liquids*, 328, 115450. doi: 10.1016/j.molliq.2021.115450.

- [42] Khudhair, N. A., Kadhim, M. M., & Khadom, A. A. (2021). Effect of trimethoprim drug dose on corrosion behavior of stainless steel in simulated human body environment: experimental and theoretical investigations. *Journal of Bio-and Tribo-Corrosion*, 7(3), 124. doi: 10.1007/s40735-021-00559-8.
- [43] Yazdanshenas, R., & Gharib, F. (2017). Spectrophotometric determination of preferential solvation and solvation shell composition of morin hydrate in some water-aliphatic alcohol mixed solvents. *Journal of Molecular Liquids*, 243, 414-419. doi: 10.1016/j.molliq.2017.08.064.
- [44] Purkayastha, D. D., & Madhurima, V. (2013). Interactions in water-THF binary mixture by contact angle, FTIR and dielectric studies. *Journal of Molecular Liquids*, 187, 54-57. doi: 10.1016/j.molliq.2013.05.024.
- [45] Bozkurt, E., GÜL, H. İ., & TUĞRAK, M. (2017). Investigation of solvent effect on photophysical properties of some sulfonamides derivatives. *Turkish Journal of Chemistry*, 41(2), 282-293. doi: 10.3906/kim-1604-61.
- [46] Delgado, D. R., & Martínez, F. (2015). Preferential solvation of some structurally related sulfonamides in 1-propanol+ water co-solvent mixtures. *Physics and Chemistry of Liquids*, 53(3), 293-306. doi: 10.1080/00319104.2014.961191.
- [47] Vibha, K., Prachalith, N. C., Reddy, R. A., Ravikantha, M. N., & Thipperudrappa, J. (2023). Computational studies on sulfonamide drug molecules by density functional theory. *Chemical Physics Impact*, 6, 100147. doi: 10.1016/j.chphi.2022.100147.
- [48] Zakrzewski G, Gao J, Rega N, Zheng G, Liang W, Hada M, Ehara M, Toyota K, Fukuda R, Hasegawa J, Ishida M, Nakajima T, Honda Y, Kitao O, Nakai H, Vreven T, Throssell K, Montgomery Jr J A, Peralta J E, Ogliaro F, Bearpark M, Heyd J J, Brothers E, Kudin K N, Staroverov V N, Keith T, Kobayashi R, Normand J, Raghavachari K, Rendell A, Burant J C, Iyengar S S, Tomasi J, Cossi M, Millam J M, Klene M, Adamo C, Cammi R, Ochterski J W, Martin R L, Morokuma K, Farkas O, Foresman J B & Fox D J. (2009) *Gaussian 09, Revision D.01*, Gaussian Inc, Wallingford, CT,.
- [49] Dennington R D , Keith T A & Millam J M. (2016) Gauss View, Version 6.0, Semichem Inc, Shawnee Mission KS.

- [50] Shrikrupa C, Patil S A, Wari M N , Mulimani B G & Inamdar S R. (2023). Dipole Moments of Coumarin 500 Dye in Aqueous Ethanol: Solvatochromic and Computational Study, *IJIRT*, 10(3), 349-353.
- [51] Adsmond, D. A., & Grant, D. J. (2001). Hydrogen bonding in sulfonamides. *Journal of pharmaceutical sciences*, 90(12), 2058-2077.
- [52] Lakowicz J R. (1983). Principles of fluorescence spectroscopy, *Springer*, New York.
- [53] Miotke-Wasilczyk, M., Józefowicz, M., Strankowska, J., & Kwela, J. (2021). The Role of Hydrogen Bonding in Paracetamol-Solvent and Paracetamol-Hydrogel Matrix, Interactions. *Materials*, 14(8), 1842. doi: 10.3390/ma14081842.